Diffusion tensor in electron transport in gases in a radio-frequency field

Kenji Maeda, Toshiaki Makabe, and Nobuhiko Nakano
Department of Electronics, Keio University, 3-14-1 Hiyoshi, Yokohama 223, Japan

Svetlan Bzenić and Zoran Lj. Petrović
Institute of Physics, University of Belgrade, P.O. Box 57, 11001, Belgrade, Yugoslavia
(Received 8 October 1996; revised manuscript received 19 December 1996)

Electron transport theory in gases in a radio-frequency field is developed in the hydrodynamic regime from the density gradient expansion method of the Boltzmann equation. Swarm parameters for the radio-frequency (rf) field with periodic time modulation are derived as functions of both reduced effective field strength and reduced angular frequency from the time dependent velocity distribution function. The rf electron transport in phase space is analyzed from the series of governing equations by a direct numerical procedure (DNP). Electron velocity distribution function and corresponding swarm parameters obtained from DNP agree with those of the Monte Carlo simulation in the frequency range 10–200 MHz at 10 Td for Reid's inelastic ramp model gas. The temporal modulation of the ensemble average of energy and the diffusion tensor are discussed. The appearance of the anomalous time behavior of the longitudinal diffusion coefficient is discussed in particular detail, and we provide an explanation of the observed effect. [S1063-651X(97)06805-0]

PACS number(s): 52.25.Dg, 51.10.+y, 52.65.−y, 52.80.Pi

I. INTRODUCTION

Knowledge of electron transport is required for the design of low temperature plasma reactors for material processings, as well as for understanding fundamental properties of nonequilibrium discharges. There are two main approaches to the theoretical description of electron transport: the kinetic Boltzmann equation [1], and stochastic particle simulation by the Monte Carlo method. A number of studies of electron transport in gases in a dc electric field have been carried out in the past few decades. The phenomenological density gradient expansion method of the velocity distribution function of electrons $g(\boldsymbol{r},\boldsymbol{v})$ was established by Kumar, Skullerud, and Robson in order to describe the transport of electrons with a density gradient in position in a uniform dc field on the basis of a hydrodynamic regime approximation [2,3]. dc electron transport theory in gases based on the microscopic molecular properties has been applied to the study of the electron swarm parameters necessary for discharge modeling and design. This theory has also been used to establish a set of absolute collision cross sections for electrons in gases. A numerical finite-difference technique not involving any expansion of the velocity distribution, $g(\boldsymbol{v},t)$, has been developed in order to study the relaxation process of dc electron swarm parameters in velocity space under the spatially independent Boltzmann equation [4,5].

Reactive plasmas maintained by radio-frequency (rf) or microwave sources have come to play an important role in the fabrication of microelectronic devices. Modeling of capacitively or inductively coupled plasmas driven by an rf source has been performed in order to elucidate the discharge structures, particularly aiming at numerical design of plasma processing reactors and procedures [6–8]. Under these circumstances, detailed investigation of the rf electron swarm transport is significant and desirable. Nevertheless, only a few studies of electron transport in rf fields have been made. The investigation of rf electron swarms with a spatially uniform density has been carried out by Wilhelm and Winkler [9] and Makabe and co-workers [10–13].

The identification of novel temporal behavior of the longitudinal diffusion coefficient in rf fields was briefly reported in Ref. [14]. This behavior is dramatically different from that of the transport coefficient in a dc field. The diffusion in a rf field has been discussed recently by White *et al.* [15] independently of our work. The definition of the anomalous diffusion effect used by these authors is narrower than ours and they employ a different numerical technique to analyze it.

At this point we should point out what we regard as anomalous. If at each moment swarm properties relax much faster than the field changes, we obtain a quasi-dc situation. The swarm parameters correspond then to the instantaneous field and can be obtained by dc calculations for the given field. Under quasi-dc conditions both diffusion coefficients are expected to become equal to the isotropic thermal coefficient as the field becomes zero. This value is much lower than the high field value for the operating conditions taken in this work. So both components of the diffusion tensor should have a minimum as the field becomes zero. At higher frequencies the minimum may become shallower as the swarm fails to relax before the field increases again. Those two possibilities constitute an expected behavior. Anomalous time dependence of the longitudinal diffusion coefficient is exactly the opposite; the longitudinal diffusion coefficient has a narrow maximum for the zero field conditions.

Another important aspect of this work is that we employ two different techniques to verify that the observed phenomenon is realistic. While we have full confidence in the adequacy of the time dependent transport theory, some may claim that assumptions built into the development of the theory may be inadequate for the rapidly varying electric fields. Thus it is particularly important to verify the results by Monte Carlo simulations (MCS), which do not suffer from similar limitations.

To the best of our knowledge, there has been no compara-

tive study elucidating all aspects of anomalous longitudinal diffusion coefficient in the rf field. Thus, a more detailed and thorough study, as well as being from a different point of view, is needed to confirm the anomalous diffusion phenomenon in rf fields.

This paper presents the electron transport theory, as derived from the kinetic Boltzmann equation, in gases in phase space and the results of Monte Carlo simulations under an rf field with periodic temporal variation. We focus particular attention on the novel temporal behavior of the electron diffusion tensor specific to the rf field. In Sec. II, we develop and formulate the rf electron transport theory on the basis of the hydrodynamic regime, using the method of the dc electron transport theory, in which the velocity distribution function is expanded into powers of the density gradient [2]. In Sec. III, various temporal properties of the rf electron transport with periodicity are shown and discussed. Finally, in Sec. IV, we identify the conditions under which the anomalous electron diffusion takes place in the rf field.

II. THEORY

The velocity distribution function of electrons in phase space $g(\boldsymbol{r},\boldsymbol{v},t)$ under an rf field can be derived from the Boltzmann equation [1],

$$\frac{\partial}{\partial t}g(\boldsymbol{r},\boldsymbol{v},t)+\boldsymbol{v}\cdot\frac{\partial}{\partial \boldsymbol{r}}g(\boldsymbol{r},\boldsymbol{v},t)+\frac{e\boldsymbol{E}(t)}{m}\cdot\frac{\partial}{\partial \boldsymbol{v}}g(\boldsymbol{r},\boldsymbol{v},t) =J[g(\boldsymbol{r},\boldsymbol{v},t)], \tag{1}$$

where, $\boldsymbol{r}$, $\boldsymbol{v}$, and t show position, velocity, and time, respectively. e and m are the electron charge and the mass, and $J[g(\boldsymbol{r},\boldsymbol{v},t)]$ the collision term between the electron and the neutral molecule. The external electric field $\boldsymbol{E}(t)$ is assumed to be uniform in position and to vary with time as follows:

$$\boldsymbol{E}(t)=\sqrt{2}E_R\boldsymbol{k}\cos(\omega t), \tag{2}$$

where E_R and ω are the root mean square value and the angular frequency of the rf field respectively, $\boldsymbol{k}$ is the unit vector in the field direction (z axis). $g(\boldsymbol{r},\boldsymbol{v},t)$ in a rf field is expanded in terms of spatial gradients of the electron number density $n(\boldsymbol{r},t)$ in a manner similar to that for the dc field [2],

$$g(\boldsymbol{r},\boldsymbol{v},t)=\sum_{k=0}^{\infty}\boldsymbol{g}^k(\boldsymbol{v},t)\odot\left(-\frac{\partial}{\partial \boldsymbol{r}}\right)^k n(\boldsymbol{r},t), \tag{3}$$

where $\boldsymbol{g}^k(\boldsymbol{v},t)$ is a tensor of rank k and $\odot$ denotes a k-fold scalar product. Each tensorial function $\boldsymbol{g}^k(\boldsymbol{v},t)$ is normalized at each time t as

$$\int \boldsymbol{g}^k(\boldsymbol{v},t)d\boldsymbol{v}=\begin{cases}1, & (k=0)\\ 0, & (k\neq 0).\end{cases} \tag{4}$$

The continuity equation for the electron number density $n(\boldsymbol{r},t)$ is expressed in terms of the density gradients with time dependent transport coefficient $\boldsymbol{\omega}^k(t)$, as follows:

$$\frac{\partial}{\partial t}n(\boldsymbol{r},t)-\sum_k \boldsymbol{\omega}^k(t)\odot\left(-\frac{\partial}{\partial \boldsymbol{r}}\right)^k n(\boldsymbol{r},t)=0, \tag{5}$$

where $\omega^0(t)$, $\boldsymbol{\omega}^1(t)$, and $\boldsymbol{\omega}^2(t)$ denote the time dependent effective ionization rate, the drift velocity vector, and the diffusion tensor, respectively. It is noted in the case of electron transport in a dc field that these transport coefficients $\boldsymbol{\omega}^k$, after finite relaxation times, are independent of time [2,4,5]. In the rf electron transport targeted by the present paper, the time dependent coefficients $\boldsymbol{\omega}^k(t)$ are essentially different from those in a dc field, due to both temporal field variation and collisional relaxation processes. Substitution of Eq. (3) in the Boltzmann equation (1) under provision of electron continuity Eq. (5) results in a series of equations with time dependent velocity distribution $\boldsymbol{g}^k(\boldsymbol{v},t)$. The first two partial differential equations are written as

$$\frac{\partial}{\partial t}g^0(\boldsymbol{v},t)+\frac{e\boldsymbol{E}(t)}{m}\cdot\frac{\partial}{\partial \boldsymbol{v}}g^0(\boldsymbol{v},t)+\omega^0(t)g^0(\boldsymbol{v},t)-J[g^0(\boldsymbol{v},t)] =0, \tag{6}$$

$$\frac{\partial}{\partial t}\boldsymbol{g}^1(\boldsymbol{v},t)+\frac{e\boldsymbol{E}(t)}{m}\cdot\frac{\partial}{\partial \boldsymbol{v}}\boldsymbol{g}^1(\boldsymbol{v},t)+\omega^0(t)\boldsymbol{g}^1(\boldsymbol{v},t)-J[\boldsymbol{g}^1(\boldsymbol{v},t)] =\boldsymbol{v}g^0(\boldsymbol{v},t)-\boldsymbol{\omega}^1(t)g^0(\boldsymbol{v},t). \tag{7}$$

Note that these equations have the same form as Eq. (28a) in the review by Kumar *et al.* [2], except for the time dependence of the velocity distribution and the transport coefficients. Taking into account the axial symmetry of $\boldsymbol{g}^k(\boldsymbol{v},t)$ with respect to the field direction $\boldsymbol{k}$, the first order velocity distribution $\boldsymbol{g}^1(\boldsymbol{v},t)$ is divided into two components, $g_L^1(\boldsymbol{v},t)$ and $g_T^1(\boldsymbol{v},t)$, parallel and perpendicular to the field $\boldsymbol{E}(t)$,

$$g_L^1(\boldsymbol{v},t)=\boldsymbol{g}^1(\boldsymbol{v},t)\cos\theta,\quad g_T^1(\boldsymbol{v},t)=\boldsymbol{g}^1(\boldsymbol{v},t)\sin\theta, \tag{8}$$

where θ is the polar angle from the v_z axis.

The macroscopic transport coefficients, i.e., effective ionization rate $R_{i_{\rm eff}}(t)$ and drift velocity $\boldsymbol{v}_d(t)$, are given by

$$R_{i_{\rm eff}}(t)=\omega^0(t)=N\int [Q_i(v)-Q_a(v)]vg^0(\boldsymbol{v},t)d\boldsymbol{v}, \tag{9}$$

$$\boldsymbol{v}_d(t)=\omega_z^1(t)=\int \boldsymbol{v}g^0(\boldsymbol{v},t)d\boldsymbol{v} +N\int [Q_i(v)-Q_a(v)]\boldsymbol{v}g_L^1(\boldsymbol{v},t)d\boldsymbol{v}, \tag{10}$$

where N is the gas number density, and $Q_i(v)$ and $Q_a(v)$ are the collision cross sections for ionization and electron attachment. The excitation rate $R_j(t)$ of a vibrationally or electronically excited state with threshold energy $\boldsymbol{\epsilon}_j$ is obtained in a manner similar to Eq. (9). The drift velocity in the electron conservative case is equal to the first term in Eq. (10), which represents the ensemble average of velocity. The second term in Eq. (10) represents the influence of the electron production and loss on the center of mass drift velocity [16]. The ensemble average of energy $\langle\boldsymbol{\epsilon}(t)\rangle$ is written as

$$\langle\boldsymbol{\epsilon}(t)\rangle=\int\frac{1}{2}mv^2g^0(\boldsymbol{v},t)d\boldsymbol{v}. \tag{11}$$

In addition, the longitudinal and transverse diffusion coefficients $D_L(t)$ and $D_T(t)$ parallel and perpendicular to the field are written as

$$\omega^2(t)=\int \boldsymbol{v}\boldsymbol{g}^1(\boldsymbol{v},t)d\boldsymbol{v}=\begin{bmatrix} D_T(t) & 0 & 0 \\ 0 & D_T(t) & 0 \\ 0 & 0 & D_L(t) \end{bmatrix}, \tag{12}$$

where

$$D_L(t)=\omega_{zz}^2(t)=\int v\ \cos\theta\ g_L^1(\boldsymbol{v},t)d\boldsymbol{v}, \tag{13}$$

$$D_T(t)=\omega_{xx}^2(t)=\omega_{yy}^2(t)=\frac{1}{2}\int v\ \sin\theta\ g_T^1(\boldsymbol{v},t)d\boldsymbol{v}. \tag{14}$$

All the time dependent transport coefficients, having periodicity, are functions of both reduced effective field strength E_R/N and reduced angular frequency ω/N, as discussed in Refs. [10,11] Both fundamental and higher-order Fourier components in time of the rf transport coefficient were studied in Refs. [10,11], with the exception of the diffusion tensor. The temporal modulation of $D_L(t)$ and $D_T(t)$ is therefore discussed in this paper in Sec. III A.

We employ a direct numerical procedure (DNP) to obtain $g^0(\boldsymbol{v},t)$ and $\boldsymbol{g}^1(\boldsymbol{v},t)$ from Eqs. (6) and (7). DNP is a finite-difference scheme using an explicit second-order upwind discretization for the velocity derivatives in spherical coordinates. In order to reduce the accumulation of error and to shorten the CPU time, our numerical algorithm, presented in the previous study [13], is now revised to include calculation in all spherical coordinates, rather than employ a coordinate transformation at each time step between the Cartesian and spherical coordinates. The present code was tested for Reid's inelastic ramp model gas [17], i.e., the electron conservative case, in a dc field, and the transport coefficients were compared with those in the literature [18]. The present results, including the diffusion coefficients, are in reasonable agreement with the previous ones within a scattering of 2% at E/N of 1, 12, and 24 Td (1 Td$=10^{-17}$ V cm^2).

The other method for investigating electron transport in rf fields is the Monte Carlo simulation. It is difficult to use the null-collision technique to determine the time of the next collision in a time-varying field in MCS [22]. We thus solve the integral equation for the collision probability discretized in small time steps, which are determined as a small fraction either of the mean free time or of the period of the rf field, depending on the conditions. Hence the present MCS is not very efficient for use in a low frequency field due to a large number of collisions during one period, which may last much longer than the time required for MCS in a dc field to fully relax and achieve good statistics. The number of time steps is determined in such a way as to optimize the performance of the MCS code without reducing the accuracy of the results. Normally a large number of electrons, 10^5, is followed simultaneously in time. The gas molecules are regarded as stationary.

The Monte Carlo code assumes isotropic scattering of electrons, which is appropriate for electrons and also assumes conservative (electron number saving) processes. Both assumptions can be relaxed to include a more complex representation of collisions. Numerical algorithms for obtaining random numbers were shown independently to satisfy all the criteria required for our simulation. The initial conditions for electrons are chosen in such a way that the approach to the final periodic state (quasiequilibrium) is not exceedingly long, but we do not attempt to speed it up by selecting the final distributions from the previous simulation. Usually a monoenergetic swarm or Maxwellian with isotropic velocity with mean energy close to but not equal to the final state is selected as the initial distribution of the swarm.

The approach to quasiequilibrium is monitored by observing the time dependence of the ensemble average of energy and of the excitation coefficients, and only after quasiequilibrium has been achieved is sampling of the required quantities commenced. Sampling is always performed at times fully uncorrelated with moments of collisions.

The MCS code has been tested in dc fields by performing calculations for Reid's inelastic ramp model gas [17] and argon, and comparing the results to the standard results from the literature [18]. Agreement within 2% was achieved for mean energies, drift velocities, and diffusion coefficients. For the Reid's ramp model all collisions are isotropic. The MCS code has two different versions; the more efficient follows the electron kinetics in velocities only. That code is used to establish ensemble average of energies, drift velocities, and collision rate coefficients. When, however, diffusion coefficients are required, the spatial distribution of the electron swarm is followed as well. The diffusion coefficients are derived from [19]

$$D_L(t)=\frac{1}{2}\frac{d}{dt}\langle[z(t)-\langle z(t)\rangle]^2\rangle, \tag{15}$$

$$D_T(t)=\frac{1}{4}\frac{d}{dt}\langle x(t)^2+y(t)^2\rangle, \tag{16}$$

where $\boldsymbol{r}(x,y,z)$ is the position space coordinates (z is along the direction of the electric field) of the test electron at time t. The time-dependent diffusion coefficients are obtained by differentiating the mean square value from the center of mass position. No particular smoothing or fitting is performed prior to differentiation. A numerically sensitive differentiation procedure may be avoided by using the following formulas:

$$D_L(t)=\langle zv_z\rangle-\langle z\rangle\langle v_z\rangle, \tag{17}$$

$$D_T(t)=\tfrac{1}{2}(\langle yv_y\rangle+\langle xv_x\rangle), \tag{18}$$

giving identical results with a somewhat better statistics.

III. RESULTS AND DISCUSSION

A. Temporal modulation of the electron transport

The present calculations by DNP and MCS are performed under identical external conditions, i.e., in Reid's ramp model gas with the mass of 4.0 amu (see Fig. 1) at 1 Torr, at effective reduced field strength $E_R/N=10$ Td and 300 K for field frequencies 100 kHz $\leqslant f\leqslant$ 200 MHz.

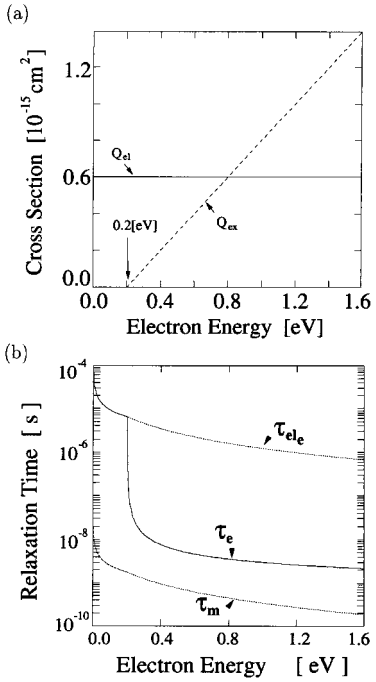

FIG. 1. Set of collision cross sections for Reid inelastic ramp model with mass of 4 amu, which is used in this study. (a) Collision cross sections; (b) collisional relaxation times at 1 Torr. Q_{el} and Q_{ex} are, respectively, the cross sections for elastic momentum transfer and for electronic excitation. τ_m and τ_e are the relaxation times for momentum and energy.

Figure 2(a) shows the time modulation of the ensemble average of energy $\langle \epsilon(t) \rangle$ obtained by DNP and MCS for frequencies of 10, 50, and 200 MHz at $E_R/N = 10$ Td. In the case of quasi-dc, shown in Fig. 2(a), we drew the relaxed steady state dc values obtained by application of the DNP technique for the instantaneous $E(t)/N$ in Eq. (2). Shapes of the modulation and of the phase delay are in good agreement within 3% errors for all frequencies, though the value obtained by MCS is systematically a little larger than that obtained by DNP. The reason is that $g^0(\boldsymbol{v},t)$ by MCS has a slightly smaller value along the axial direction (v_z) than that by DNP (see Fig. 3 at $\omega t = 0$ and $\pi/2$). Possible causes for this are differences in interpolation procedures for cross sections. The differences are, however, within the statistical scatter of the data and thus overall agreement between the two techniques is good.

The ensemble average of energy $\langle \epsilon(t) \rangle$ has a harmonic of 2ω as the fundamental wave and, further, smaller even harmonics [10,11]. The phase delay increases and the amplitude of the time modulation decreases with increasing field frequency at a constant E_R/N. It is noteworthy that the phase lag during the period when the field is weak is larger than when the field is large. This phenomenon is due to the dependence of the energy relaxation time on both collision type and rate as a function of electron energy (see Fig. 1), so that relaxation time shortens with an increase in energy for most gases [10,11,20].

Figure 2(b) shows the time variation in the longitudinal and transverse diffusion coefficients, $D_L(t)$ and $D_T(t)$, obtained by DNP (lines) and MCS (points) for $E_R/N = 10$ Td, $f = 10$, 50, and 200 MHz at 1 Torr and 300 K. The diffusion coefficients by MCS are calculated both from the time derivative of the variance in $n(z,t)$, Eqs. (15) and (16), and also by using Eqs. (17) and (18) with insignificant differences. The results for diffusion coefficients obtained by DNP and MCS (see Fig. 2) are in very good agreement, though the calculations by MCS contain statistical scatter.

Figure 4 shows the frequency dependence of dc components of $\langle \epsilon(t) \rangle$, $ND_L(t)$, and $ND_T(t)$ at a constant value of $E_R/N = 10$ Td. $\langle \epsilon \rangle_{\mathrm{dc}}$ has a broad peak as a function of applied frequency. The peak originates from the relation between the collisional relaxation time of energy and the period of the applied field. That is, the minimum value of $\langle \epsilon(t) \rangle$ gradually increases with increasing field frequency, while the maximum remains constant [Fig. 2(a)], because the electrons first lose their ability to relax the energy during the lower field phase. This leads to a gradual rise in the time-averaged mean energy $\langle \epsilon \rangle_{\mathrm{dc}}$ as a function of applied frequency. When the frequency is further increased, there is no longer time to gain sufficient energy from the instantaneous field, and the maximum of $\langle \epsilon(t) \rangle$ begins to decrease. This results in a drop of both the time-averaged energy and the temporal modula-

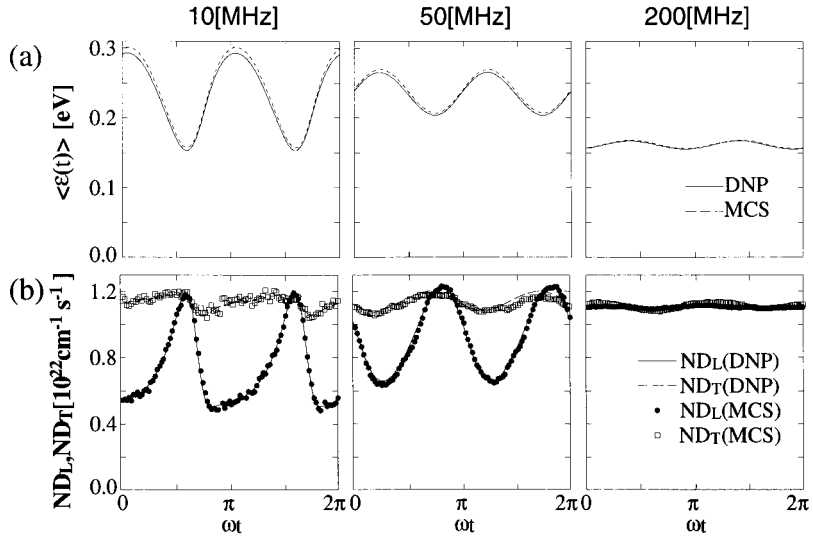

FIG. 2. Time modulations of (a) ensemble average of energy $\langle \epsilon(t) \rangle$, and (b) longitudinal and transverse diffusion coefficients $D_L(t)$ and $D_T(t)$, obtained by DNP (solid line) and MCS (dashed line) for $E_R/N = 10$ Td, $f = 10$, 50, and 200 MHz at 1 Torr in Reid inelastic ramp model gas.

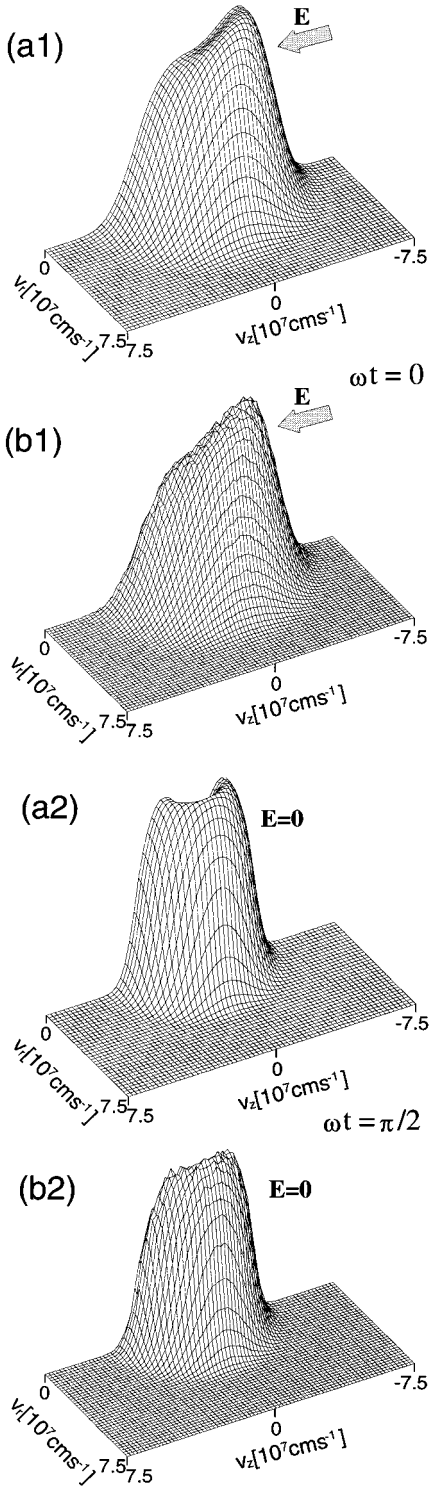

FIG. 3. Temporal structure of zeroth-order velocity distribution $g^0(\boldsymbol{v},t)$ at $\omega t = 0$ and $\pi/2$ by (a) DNP and (b) MCS for $E_R/N =$ 10 Td, $f = 10$ MHz at 1 Torr in Reid inelastic ramp model gas.

tion. As a result, $\langle \epsilon \rangle_{\rm dc}$ usually reaches its maximum for very high frequencies (VHF). A momentum transfer theory argument for the presence of the maximum in $\langle \epsilon \rangle_{\rm dc}$ was given in Ref. [23]. The frequency characteristics of the rf transport coefficients relating to the zeroth order velocity distribution $g^0(\boldsymbol{v},t)$ are discussed in detail in our previous papers [10,11,13].

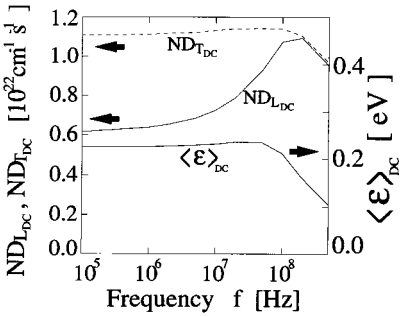

FIG. 4. Frequency dependence of the dc components of $\langle \epsilon(t) \rangle$, $ND_L(t)$ and $ND_T(t)$ at $E_R/N = 10$ Td and 1 Torr as a function of external frequency in Reid inelastic ramp model gas.

The dc value of the transverse diffusion coefficient, $D_{T_{\rm DC}}$, has frequency characteristics similar to those of $\langle \epsilon \rangle_{\rm dc}$, which suggests that $D_{T_{\rm DC}}$ reflects the characteristics of the time-averaged energy (see Fig. 4). As the field frequency increases, the dc value of the longitudinal diffusion coefficient, $D_{L_{\rm DC}}$, also increases to a sharp peak at 200 MHz. For higher frequencies $D_{L_{\rm DC}}$ asymptotically approaches $D_{T_{\rm DC}}$, which monotonically decreases due to the reduction of the energy gained from the field. These monotonically decreasing characteristics of the rf transport coefficients as a function of field frequency reflect the strong influence of *electron trapping* by very high frequency electric field. Under those conditions, the electron diffusion becomes isotropic.

It is also worth noticing that $D_L(t)$ in the quasi-dc, converges asymptotically to a thermal value when the field approaches zero [21,22], whereas the results for rf fields show a peak in this phase. This feature of the rf field indicates that electrons cannot relax their energy at this phase but also that some other process occurs that causes a peak in $D_L(t)$. The temporal profile of $D_L(t)$ in the rf field is anomalous, and is completely different from that in the case of the expected behavior. The characteristics of the modulation and the phase lag in $D_L(t)$ are different from those of $D_T(t)$.

B. Mechanism of anomalous diffusion in rf field

Figure 5 schematically describes the anomalous diffusion of electrons $D_L(t)$ during one short period A overlapping with the zero crossing of the electric field. At the same time

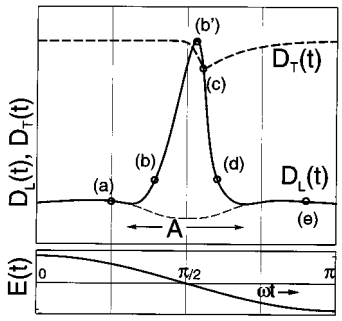

FIG. 5. Schematic diagram of temporally modulated diffusion coefficients, $D_L(t)$ and $D_T(t)$ with periodicity of π in the rf field. A denotes the period of the phase of anomalous diffusion (see text).

$D_T(t)$ does not show anomalous time dependence. It is known from the electron transport in dc fields that $D_L < D_T$ is satisfied for Reid's inelastic ramp model gas for all E/N [17]. We have to consider the distributions in both velocity and position spaces during one period in order to investigate the temporal behavior of the diffusion fluxes. Figure 6 describes schematically the axial components of the first-order velocity distribution $g_L^1(\boldsymbol{v},t)$ and density distribution $n(z,t)$ at each phase in Fig. 5, as related to the diffusion flux in the axial direction,

$$\Gamma_{D_L}(t) = -D_L(t)\frac{\partial n(t)}{\partial z} = -\left(\int v\ \cos\theta\ g_L^1(\boldsymbol{v},t)d\boldsymbol{v}\right)\frac{\partial n(t)}{\partial z}. \tag{19}$$

Equation (19) illustrates that each component, Γ_{I} to Γ_{IV}, in the longitudinal diffusion flux is constructed by the velocity components labeled I–IV in Fig. 6. In particular, regions II and III in $g_L^1(\boldsymbol{v},t)$ in Fig. 6 form the antidiffusion components in $D_L(t)$. The ensemble average of energy $\langle \epsilon(z,t)\rangle$ at each phase ωt in Fig. 5 is also drawn schematically in Fig. 6, where ϵ_x gives the lower limit at which electrons can immediately relax to the energy corresponding to the instantaneous local field. ϵ_x is dependent on both E_R/N and ω/N, in addition to the dependence on collisional relaxation times for energy and momentum expressed by [10,11,20]

$$\tau_e^{-1}(\epsilon) = N\left[\frac{2m}{M}\nu_m(\epsilon) + \nu_j(\epsilon)\right], \tag{20}$$

$$\tau_m^{-1}(\epsilon) = N[\nu_m(\epsilon) + \nu_j(\epsilon)]. \tag{21}$$

Here M is the molecular mass, $\nu_m(\epsilon)$ and $\nu_j(\epsilon)$ are the collisional frequencies of the momentum transfer and the inelastic scattering, respectively. $\mathbf{V}_d$ in Fig. 6 indicates the direction of migration of the center of mass of $n(z,t)$. We also define the head of the swarm as the group of electrons within the spatial distribution that is at the front of the moving swarm. The tail is the group that is at the opposite end of the spatial distribution. In rf fields, unlike the dc fields, the direction of field changes and therefore the identity of the head and tail changes.

At the phase (a) when the instantaneous field of Eq. (2) is high, the local spatially dependent mean energy $\langle \epsilon(z,t)\rangle$ is higher than ϵ_x for all positions. In other words, the local energy is immediately subjected to the instantaneous field $E(t)$. Also, the value at the head of $n(z,t)$ is greater than at the tail. Then, $(\Gamma_{\mathrm{I}}+\Gamma_{\mathrm{III}}) > (\Gamma_{\mathrm{II}}+\Gamma_{\mathrm{IV}})$ and a negative slope of $g_L^1(\boldsymbol{v},t)$ at $v=0$ are satisfied owing to a higher drift flow under the external field. At this phase, $D_L(t)$ behaves nearly as it does in the dc field.

When the external field decreases [Fig. 5(b)], electrons first fail to relax their energy at the tail of the swarm, although the momentum relaxation is completely realized in a very short time, i.e., $\tau_m \ll \pi/\omega$ [see Fig. 6(b)]. The relaxation then continues towards the head of the swarm. At this point, the electrons in the tail continue to maintain a higher energy than the electrons in the dc field (equal to the instantaneous rf field). Then, Γ_{IV} increases more than does the value in the dc field. It corresponds to a positive slope of $g_L(\boldsymbol{v},t)$ at $v=0$. $D_L(t)$ in phase (b) has a larger value than in phase (a), as shown in Fig. 5.

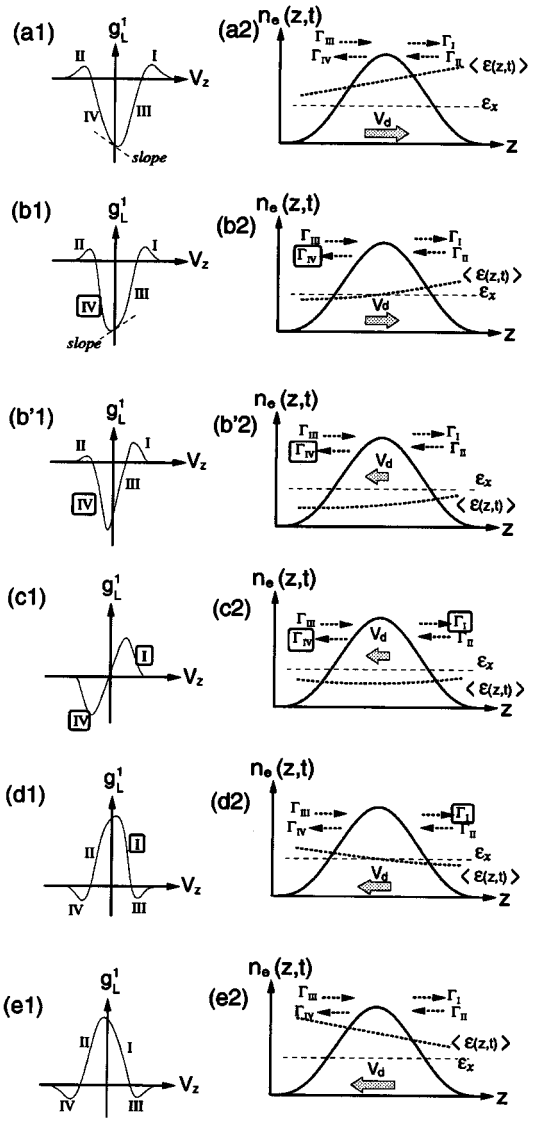

FIG. 6. Schematic diagram of the distributions in both velocity and position spaces, relative to the diffusion flux parallel to the field. (a)–(e) correspond to each phase in Fig. 5.

After the rf field crosses the zero value at $\omega t = \pi/2$, the direction of motion quickly changes because the momentum relaxes rapidly, while the energy does not relax [Fig. 6(b')] because elastic collisions are not efficient in energy exchange. As a result, the slope of $\langle \epsilon(z,t)\rangle$ is still positive along the z axis. Then, the new front with the energy of less than $\langle \epsilon(t)\rangle$ at $\omega t = \pi/2$ will be first accelerated by the field in the subsequent phase. The tail will also maintain its energy, which is higher than that of the head. This means that the total flux, which is the sum of drift and thermal fluxes, increases toward the left. The result is a continued increase of $D_L(t)$, and the relation $D_L(t) > D_T(t)$. For phase (c), components II and III, in $g_L^1(\boldsymbol{v},t)$ are negligible and it appears as a transit from the phase (b) to (d).

The phase (d) in Figs. 5 and 6 corresponds to phase (b) with the opposite drift direction. In phase (d), owing to the

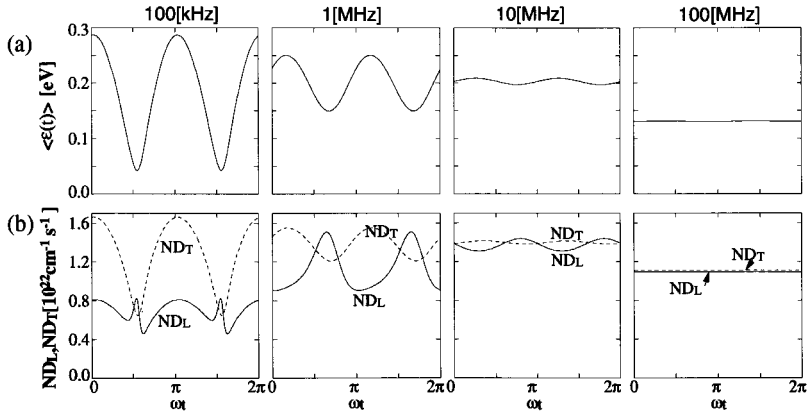

FIG. 7. Temporal modulations of (a) $\langle \epsilon(t) \rangle$, and (b) $ND_L(t)$ and $ND_T(t)$ for $E_R/N = 1.5$ Td, $p = 1$ Torr, and $f = 100$ kHz, 1 MHz, 10 MHz, and 100 MHz in the model gas with $Q_m = 6 \times 10^{-16}$ cm^2 and mass of 0.4 amu.

acceleration by the field, $\langle \epsilon(z,t) \rangle$ relaxes at the front to the value corresponding to the instantaneous field, while in the tail it does not. The number of electrons with energy equivalent to the instantaneous field gradually increases from the head to tail. D_L here approaches the value for the corresponding dc field. At phase (e), the temporal profile of D_L coincides with that in the dc field equal to the amplitude of the rf field, because the energy is completely relaxed to the field value.

In addition to Reid's inelastic ramp model, we studied the anomalous diffusion in the model gas with only a constant momentum transfer cross section, $Q_m = 6 \times 10^{-16}$ cm^2, and molecular mass of 0.4 amu. for $E_R/N = 1.5$ Td and 100 kHz $< f <$ 100 MHz at 1 Torr. Relaxation to the quasiequilibrium in MCS is very long for this model so we only present DNP results. The presence of the anomalous diffusion is confirmed again in Fig. 7, even in the system without excitation. This shows that the first requirement for the anomalous diffusion is the decreasing collisional energy relaxation time τ_e with energy. In fact, the novel phenomenon in $D_L(t)$ is not present in the system where τ_e is independent of electron energy. In the rf electron transport with a constant τ_e, of course, $D_L(t)$ is equal to $D_T(t)$ during one period, as it is in the dc field [21,22].

At this point we should address the results of White *et al.* [15]. These authors limit the definition of anomalous effect only to the overshoot of the transverse diffusion coefficient by the longitudinal diffusion coefficient, i.e., $D_L(t) > D_T(t)$. We, however, regard both aspects of the behavior of longitudinal diffusion as anomalous. The first is the increase rather than decrease of the coefficient in the region *A* in Fig. 5. While one would expect a small increase in $D_L(t)$ with decreasing field due to the quasi-dc E/N dependence, the increase starting between points (a) and (b) is unexpected and therefore anomalous. In quasi-dc one would expect both coefficients to rapidly decrease towards the equal thermal value when the field goes through zero. At high frequencies, finite relaxation time would make the modulation of diffusion coefficients smaller but an increase is unexpected. In that sense transverse diffusion shows a more regular behavior. The second aspect of the diffusion anomaly is that for an even narrower period of time the longitudinal diffusion coefficient is larger than the transverse diffusion coefficient as discussed by White *et al.* Our results and explanations are fully consistent with those of White *et al.*

A simple general explanation of the first aspect of the rf diffusion anomaly can be proposed on the basis of Fig. 3. For a finite electric field [(a1) and (b1)] the velocity distribution function in the longitudinal direction peaks off center and is narrower than the symmetric distribution in the transverse direction. When the field is equal to zero, $E = 0$, a very rapid momentum relaxation redirects the velocities while the energy relaxation is small. This leads to a symmetric distribution in both directions that is equivalent to the equality of the two diffusion coefficients. In other words, $D_L(t)$ has to increase because momentum was relaxed rapidly, leading to redirectioning of the velocity. At the same time, energy has not relaxed in such a short time. Resulting symmetric velocity distribution is equivalent to isotropic diffusion. The overshoot $D_L(t) > D_T(t)$ occurs for a brief period when field changes sign. At that instant the head of the swarm from the previous half period becomes the tail while still continuing to expand in the original direction. The new head (which was up to that moment the tail) has a lower energy so it can be more easily accelerated in the new direction of the field. The transverse direction does not have such acceleration and thus the spread of the velocities is smaller, i.e., diffusion is slower. Such a situation ends when the new tail decreases in mean velocity and the number and distribution become more isotropic again with a tendency to develop towards the asymmetric dc-like distribution with $D_T(t) > D_L(t)$.

Anomalous longitudinal diffusion in rf fields may be disregarded by some as an effect that is difficult to observe experimentally. However, even at present there are facilities to observe the effect. The so-called Cavalleri diffusion experiment was developed to measure the electron diffusion coefficients directly, and it is possible to operate it with an rf field [24]. At present the time averaged diffusion would be observed but it is also possible to record the time variation of the spatial profile of the electron swarm that would be phase dependent. This could be accomplished by triggering spatially resolved emission detection in conjunction with the standard Cavalleri technique. In addition to being observable by the present day techniques the anomalous diffusion is of great importance in modeling of the rf discharges and in understanding their kinetics. Anomalous longitudinal diffusion adds a degree of nonlinearity to the rf discharge models and, as can be seen from the present paper, it is quite a general phenomenon, occurring in most gases.

IV. CONCLUSION

Electron transport theory with periodic time variation in a radio-frequency field has been developed on the basis of the

kinetic Boltzmann equation in the hydrodynamic regime. The temporal profile of the electron diffusion tensor during one period under an rf field has been investigated by direct numerical procedure of the Boltzmann equation and by a stochastic Monte Carlo simulation. Of particular significance for the rf diffusion tensor is the appearance of an anomalous longitudinal diffusion. In summary, the anomalous longitudinal diffusion coefficient of electrons arises from the following conditions: (1) The total collision frequency is an increasing function of energy, i.e., $(\partial/\partial\epsilon)\tau_m(\epsilon)^{-1}>0$. (2) The relaxation of momentum transfer by collisions is very fast as compared to the rf field period, i.e., $\tau_m(\epsilon)\ll\omega^{-1}$. (3) A lack of collisional energy relaxation occurs within a limited time interval centered around the phase when the external field $E(t)$ crosses zero value. (4) In particular, electrons fail to relax the energy of their tail, which has a higher energy than the head, at the same time the head of the distribution gains energy rapidly.

That is, during the phase between (b) and (d) in Fig. 5 a unique kinetic phenomenon occurs in the isolated electron swarm in an rf field, longitudinal diffusion coefficient $D_L(t)$ has a maximum rather than the expected minimum, and even becomes larger than $D_T(t)$.

ACKNOWLEDGMENTS

We would like to thank R.E. Robson for his helpful input. This work was supported by a Grant-in-Aid for the Monbusho International Scientific Program, No. 08044169, and Keio University Special Grant-in-Aid for Innovative and Collaborative Research Project. Two of the authors (Z.Lj.P and S.B) are also grateful to the Ministry of Science and Technology of Serbia for partial support.

[1] S. Chapman and T.G. Cowling, *The Mathematical Theory of Non-Equilibrium Gases* (Cambridge University Press, Cambridge, 1970).
[2] K. Kumar, H.R. Skullerud, and R.E. Robson, Aust. J. Phys. **33**, 343 (1980).
[3] K. Kumar, Phys. Rep. **112**, 319 (1984).
[4] K. Kitamori, H. Tagashira, and Y. Sakai, J. Phys. D **11**, 283 (1978); **13**, 535 (1980).
[5] P.J. Drallos and J.M. Wadehra, J. Appl. Phys. **63**, 5601 (1988); Phys. Rev. A **40**, 1967 (1989).
[6] J.P. Boeuf, Phys. Rev. A **36**, 2782 (1987); J.P. Boeuf, Ph. Belenguer, and T. Hbid, Plasma Sources Sci. Technol. **3**, 407 (1994).
[7] T. Makabe, N. Nakano, and Y. Yamaguchi, Phys. Rev. A **45**, 2520 (1992); N. Nakano, N. Shimura, Z. Lj. Petrovic, and T. Makabe, Phys. Rev. E **49**, 4455 (1994).
[8] P.L.G. Ventzek, T.J. Sommerer, R.J. Hoekstra, and M.J. Kushner, Appl. Phys. Lett. **63**, 605 (1993); P.L.G. Ventzek, R.J. Hoekstra, and M.J. Kushner, J. Vac. Sci. Technol. B **12**, 461 (1994).
[9] J. Wilhelm and R.J. Winkler, J. Phys. (Paris) Colloq. **40**, C7-251 (1979).
[10] T. Makabe and N. Goto, J. Phys. D **21**, 887 (1988).
[11] N. Goto and T. Makabe, J. Phys. D **23**, 686 (1990).
[12] K. Maeda and T. Makabe, Jpn. J. Appl. Phys. **33**, 4173 (1994).
[13] K. Maeda and T. Makabe, Phys. Scr. **T53**, 61 (1994).
[14] K. Maeda and T. Makabe, in Europhysics Conference Abstracts **18E**, 151 (1994); in *Proceedings of the 17th International Symposium on the Physics of Ionized Gases, Belgrade, Yugoslavia, 1994* (unpublished).
[15] R.D. White, R.E. Robson, and K.F. Ness, Aust. J. Phys. **48**, 925 (1995).
[16] H. Tagashira, Y. Sakai, and S. Sakamoto, J. Phys. D **10**, 1051 (1977).
[17] I.D. Reid, Aust. J. Phys. **32**, 231 (1979).
[18] K. Ness and R.E. Robson, Phys. Rev. A **34**, 2185 (1986).
[19] H.R. Skullerud, Aust. J. Phys. **27**, 195 (1974).
[20] *Gaseous Electronics and Its Applications*, edited by R.W. Crompton, M. Hayashi, D.E. Boyd, and T. Makabe (Kluwer Academic, Dordrecht, 1991).
[21] J.H. Parker, Jr. and J.J. Lowke, Phys. Rev. **181**, 290 (1969); J.J. Lowke and J.H. Parker, Jr., *ibid.* **181**, 302 (1969).
[22] H.R. Skullerud, J. Phys. B **2**, 696 (1969).
[23] R.E. Robson, K. Maeda, T. Makabe, and R.D. White, Aust. J. Phys. **48**, 335 (1995).
[24] G. Cavalleri, Phys. Rev. **179**, 186 (1969).